JVSTB
JOURNAL OF VACUUM SCIENCE AND TECHNOLOGY B

Nanometer characterization of single point diamondturned mirrors on the micrometer and submicrometer scale

J. Yu, L. Hou, W. Sh. Ma, J. L. Cao, J. Y. Yu et al.

Citation: J. Vac. Sci. Technol. B **12**, 1835 (1994); doi: 10.1116/1.587650
View online: http://dx.doi.org/10.1116/1.587650
View Table of Contents: http://avspublications.org/resource/1/JVTBD9/v12/i3
Published by the AVS: Science & Technology of Materials, Interfaces, and Processing

Related Articles

Compact slanted comb two-axis micro-mirror scanner fabricated by silicon-on-insulator micromachining
J. Vac. Sci. Technol. B 29, 042001 (2011)

Inhibition of carbon growth and removal of carbon deposits on extreme ultraviolet lithography mirrors by extreme ultraviolet irradiation in the presence of water, oxygen, or oxygen/ozone mixtures
J. Vac. Sci. Technol. B 29, 011030 (2011)

Design and fabrication of optical thin films for remote sensing instruments
J. Vac. Sci. Technol. A 28, 867 (2010)

Complete reversal imprinting for fabricating microlens arrays with faithful shape replication
J. Vac. Sci. Technol. B 27, 2781 (2009)

Optimization of focused ion beam performance
J. Vac. Sci. Technol. B 27, 2654 (2009)

Additional information on J. Vac. Sci. Technol. B

Journal Homepage: http://avspublications.org/jvstb
Journal Information: http://avspublications.org/jvstb/about/about_the_journal
Top downloads: http://avspublications.org/jvstb/top_20_most_downloaded
Information for Authors: http://avspublications.org/jvstb/authors/information_for_contributors

ADVERTISEMENT

Nanometer characterization of single point diamond-turned mirrors on the micrometer and submicrometer scale

J. Yu
State Key Laboratory of Applied Optics, Changchun Institute of Optics and Fine Mechanics, Academia Sinica, Changchun 130022, People's Republic of China and Beijing Laboratory of Electron Microscopy, Academia Sinica, Beijing 100080, People's Republic of China

L. Hou
Jilin University of Technology, Changchun 130025, People's Republic of China, and Beijing Laboratory of Electron Microscopy, Academia Sinica, Beijing 100080, People's Republic of China

W. Sh. Ma and J. L. Cao
State Key Laboratory of Applied Optics, Changchun Institute of Optics and Fine Mechanics, Academia Sinica, Changchun 130022, People's Republic of China

J. Y. Yu
Jilin University of Technology, Changchun 130025, People's Republic of China

J. E. Yao
Beijing Laboratory of Electron Microscopy, Academia Sinica, Beijing 100080, People's Republic of China

(Received 9 August 1993; accepted 15 February 1994)

Single point diamond turning (SPDT) is one of the nanometer machining methods. We deal with the nanometer characterization of diamond-turned mirrors on the micrometer and submicrometer scale with our three-dimensional roughness measuring system based on scanning tunneling microscopy. We have studied the results of amplitude spectral density functions for these surfaces. Finally, we have calculated the total integrated scattering as a function of incident light wavelength λ and root mean square surface roughness σ and the diffracted angle θ_d as a function of the λ and the surface spatial wavelength λ_{sp}. All these measurement results are the basis for improving the SPDT surface quality.

I. INTRODUCTION

Single point diamond turning (SPDT) was used during the 1960s at government laboratories in the United States to fabricate ultraprecise machined parts and high-energy laser mirrors, but it was not until the mid-1970s that industry became involved.[1–4] At present, the surface quality is limited by the faint residual machining marks, which cause scatter that is generally unacceptable at short wavelengths, but is usually no problem in the infrared. Diamond turning of suitable materials (copper, electroless nickel, and aluminum) can generate high accuracy mirrors and aspheric optics rapidly and repeatedly at a cost significantly below that of conventional lapping and polishing methods.[3,5–7] The most important thing is how to reduce the periodic marks formed by tool feed and other roughness components formed by the machine tool vibration, unsteadiness of chip forming, and material impurity to reduce the large or small-angle scattering. The roughness structure of SPDT surfaces above the ten micrometers scale may be detected by the stylus profilers and noncontact optical profilers; but for the fine roughness structure on the micrometer and submicrometer scale we must have the aid of scanning tunneling microscopy (STM)[8,9] and atomic force microscopy,[10,11] which extend the lateral resolution to atomic dimensions and are nondamaging. It is the fine roughness structure (several nanometers in height) that affects the SPDT technology applied in short wavelength optics. The ultimate aim of developing SPDT technology is to reduce the fine roughness structure. Dragaset *et al.*[12,13] have done some earlier work on STM measurements of a diamond-turned surface. These measurements yielded information necessary for gaining a complete understanding of the diamond-turning process. In this paper, we use our three-dimensional (3D) roughness measuring system[14,15] based on STM to analyze the nanometer characterization of SPDT mirrors on the micrometer and submicrometer scale, and we study the results of amplitude spectral density (ASD) functions for these surfaces. Finally, we calculate the total integrated scattering (TIS) as a function of the incident light wavelength λ and root mean square (rms) surface roughness σ and the diffracted angle θ_d as a function of the incident light wavelength λ and the surface spatial wavelength λ_{sp}.

II. SAMPLE PREPARATION AND EXPERIMENTAL PROCEDURE

The sample material is oxygen-free high-conductivity copper (OFHC), 99% copper. The diamond-turned specimen was fabricated in a MSG-325 two axis diamond tool lathe made by Pneumo Precision, Inc.[16] Perhaps one of the most important parts of a diamond machine system is the diamond tool used for cutting. The cutting tool used for the test is made of a single-crystal diamond with a nose radius R of 1.524 mm, an edge radius ρ of 0.1 μm, a rake angle of 0°, and a clearance angle of 6°. The cutting conditions are taken as in Table I. Let the feed rate f_e be 0.6 and 1 μm/rev, respectively. We study the characterization of the roughness structure on the micrometer and submicrometer scale with our 3D roughness measuring system based on STM developed in the Beijing Laboratory of Electron Microscopy.

 0734-211X/94/12(3)/1835/4/$1.00

TABLE I. Cutting conditions.

Tool	Round nose tool (Single crystal diamond)
Work piece	OFHC
Spindle speed n	1000 rpm
Feed rate f_e	0.2, 0.4, 0.6, 0.8, 1, 1.5, and 2 μm/rev
Depth of cut a_p	1 μm
Cutting fluid	White kerosene

III. EXPERIMENTAL RESULTS AND DISCUSSION

Figure 1 shows the measuring results of the SPDT surface with the feed rate of 0.6 μm/rev. The mark spacing corresponding to 0.6 μm/rev is the primary form of the surface roughness structure. However, there are also roughness components between the two marks which may be caused by the machine tool vibration, unsteadiness of the cutting chip, and imperfection of the diamond tool [see the arrow in Fig. 1(a)]. Its horizontal scale is less than 0.6 μm. It is difficult to detect the submicrometer roughness structure with the present measuring methods. Figure 2 shows the profile of the same surface (f_e=0.6 μm/rev) with a 12.5 μm radius stylus profiler[17] and a lateral resolution much larger than 0.6 μm. So the surface features of 0.6 μm and less can not be obtained with the stylus of radius 12.5 μm. But the fine structure can be seen between the two marks in the STM image, shown in Fig. 1(a), and its 3D roughness evaluating parameters are as shown in Fig. 1(b). Machined or etched Pt–Ir tips used in the STM are characterized to an apex diameter of ~1 μm.[14]

Consider a profile signal $Z(x)$ with a Fourier transform:[18]

$$F(f_{sp})=\int_0^\infty Z(x)\exp[-j(2\pi f_{sp}x)]dx \tag{1}$$

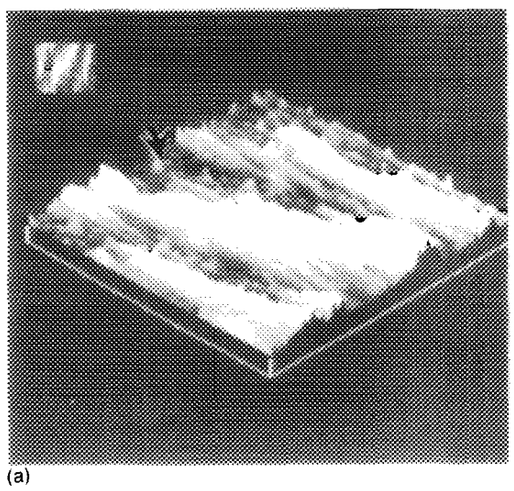

FIG. 1. Results of 3D surface measurements obtained with our 3D roughness measurement system based on STM. Scanned area is 1497.6 nm×1497.6 nm, tip bias is 50 mV, and tunnel current is 2.06 nA. (a) Image of the 3D surface; (b) 3D roughness results of the surface.

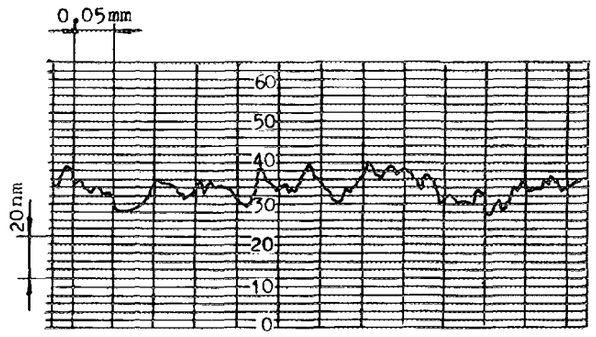

FIG. 2. Surface profile of the SPDT sample, f_e=0.6 μm/rev, obtained with Talystep profiler (see Ref. 17), measured by L. Sh. Xue. The surface is similar to that shown in Fig. 1.

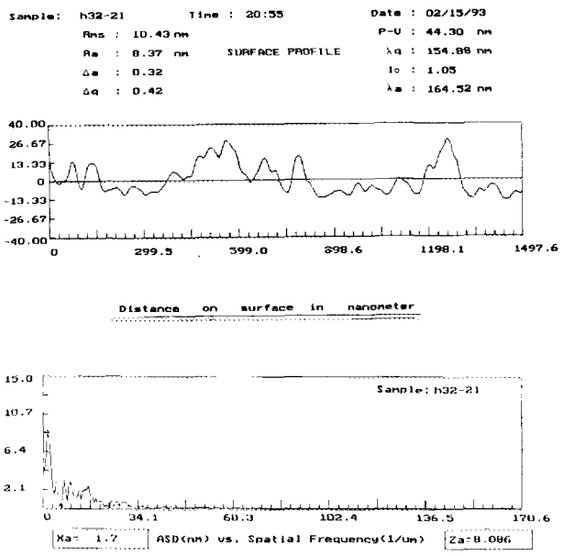

FIG. 3. Surface profile and its ASD function. The surface is similar to that shown in Fig. 1. (a) Surface profile; (b) ASD function.

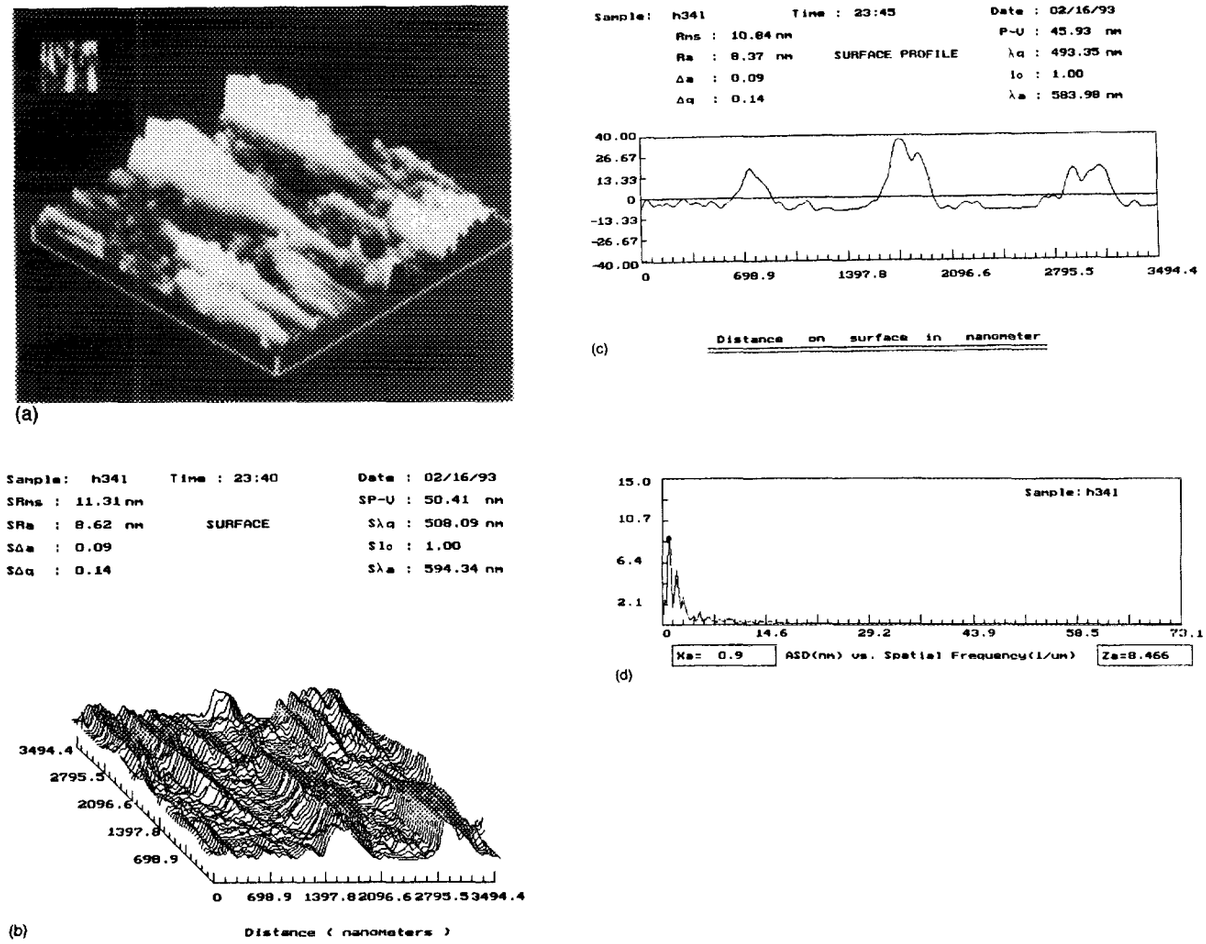

FIG. 4. Surface measurement results obtained with our 3D roughness measurement system based on STM. Scanned area is 3494.4 nm×3494.4 nm, tip bias is 50 mV, and tunnel current is 2.06 nA. (a) image of the 3D surface; (b) 3D roughness results of the surface; (c) surface profile; (d) ASD function of the (c) profile.

where $F(f_{sp})$ is band limited with spatial frequency f_{sp}, $1/\mu$m, According to Parseval equation,[19] then consider

$$\int_0^\infty Z^2(x)dx = \int_0^\infty |F(f_{sp})|^2 \, df_{sp} \tag{2}$$

where $|F(f_{sp})|^2$ is the power density function and $|F(f_{sp})|$ is the ASD function. The ASD function is of particular interest in the study of periodic surfaces, such as those produced by single point diamond turning. It can give valuable information about the tool feed rate, depth of cut, and most importantly, vibrations or other imperfections in the diamond-turning machine. The ASD function shown in Fig. 3(b) was calculated from surface-profile data [Fig. 3(a)] taken with our 3D roughness measuring system based on STM. There is a peak value at spatial frequency f_{sp1} of 1.70 μm^{-1}, which corresponds to a rms roughness σ_1 of 8.09 nm. The spatial wavelength λ_{sp2} is 0.59 nm, $\lambda_{sp2}=1/f_{sp1}$, which is equal to the tool feed rate f_e of 0.6 μm/rev approximately, implying that the 0.6 μm roughness structure was caused by the tool feed rate f_e and is the most important roughness component, or the so-called chief frequency roughness. The other peak values are as follows: $f_{sp2}=4.77$ μm^{-1} ($\lambda_{sp2}=0.2$ μm), $\sigma_2=2.73$ nm; $f_{sp3}=7.84$ μm^{-1} ($\lambda_{sp3}=0.1$ μm), $\sigma_3=2.94$ nm; $f_{sp4}=9.89$ μm^{-1} ($\lambda_{sp4}=0.1$ μm), $\sigma_4=2.94$ nm; $f_{sp5}=16.03$ μm^{-1} ($\lambda_{sp5}=0.06$ μm), $\sigma_5=2.52$ nm, and $(\sigma_1^2+\sigma_2^2+\sigma_3^2+\sigma_4^2+\sigma_5^2)^{1/2}=9.83$ nm, approximately being equal to the total rms roughness θ_G of 10.43 nm shown in Fig. 3(a), implying that these five peak values represent the important components of the surface roughness. As for which factors caused these roughness components, we have to check the machine tool and the diamond tool in detail. For example, we may diagnose the frequency of the machine tool chatter by means of frequency spectrum analyzing, and check whether the chatter frequency corresponds to the roughness components that appeared in the ASD function profile. Therefore, the ASD function of SPDT surfaces presented by us is the basis for improving the surface quality.

Figure 4 shows some measuring results for a diamond-turned OFHC surface with the feed rate of 1 μm/rev. There is a roughness structure on the surface not only on the submi-

TABLE II. Calculated TIS as a function of the wavelength λ and rms surface roughness σ and calculated θ_d as a function of the wavelength λ and the surface spatial wavelength λ_{sp}.

λ (μm)	Light source	λ_{sp} (μm)	σ (nm)	TIS	θ_d (deg)
10.6	CO_2 laser (infrared)	0.6	8.09	9.2×10^{-5}	
		1	8.47	1.0×10^{-4}	
0.6328	He–Ne laser (visible)	0.6	8.09	2.5×10^{-2}	
		1	8.47	2.8×10^{-2}	39.2
0.160	Duterium arc (EUV)	0.6	8.09	3.32×10^{-1}	15.5
		1	8.47	3.58×10^{-1}	9.2

crometer scale, $f_{sp2}=2.19\ \mu m^{-1}$, $\lambda_{sp2}=0.5\ \mu m$, $\sigma_2=5.46$ nm, but also on the micrometer scale, $f_{sp1}=0.9\ \mu m^{-1}$, $\lambda_{sp1}=1\ \mu m$, $\sigma_1=8.47$ nm.

In addition, the so-called "scalar scattering theory"[20,21] relates the specular reflectance R_s of a surface and total reflectance R_0 (which includes the diffuse reflectance R_d) to the rms surface roughness σ and incident wavelength λ:[21]

$$R_s/R_0=\exp[-(4\pi\sigma\cos\theta_0/\lambda)^2] \quad (3)$$

where θ_0 is the angle of incidence of light on the surface. If we use the TIS instrument,[22] the rms roughness is then calculated from the TIS using a rewritten form of Eq. (3):

$$\mathrm{TIS}=R_d/R_0=(R_0-R_s)/R_0=1-\exp[-(4\pi\sigma/\lambda)^2] \quad (4)$$

assuming the light to be normally incident on the surface. If TIS measurements are used to obtain a value for the effective rms roughness, the surface spatial wavelength range included in the measurement depends on the wavelength of the incident light, the angle of incidence, and the minimum and maximum collection angles of the instrument.[23] It can be calculated from the diffraction grating equation,[22] where only the first diffracted order needs to be considered if the roughness amplitude is much less than the light wavelength λ:

$$\lambda=\lambda_{sp}(\sin\theta_0\pm\sin\theta_d) \quad (5)$$

where λ_{sp} is the groove spacing (surface spatial wavelength), θ_0 the angle of incidence, and θ_d the angle of diffraction. If the incident light and diffracted light are on one side, we select "+" in Eq. (5). As an example, we calculated the TIS and diffracted angle θ_d for normally incident light with different wavelengths, as shown in Table II. Analyzing the calculated results, we know that the micrometer and submicrometer roughness structure on the SPDT surface is one of the most important factors affecting the SPDT mirror applied in visible, extreme ultraviolet (EUV), and soft x-ray regions. The roughness components in different spatial frequencies produce the different scattering, which is determined by the incident light wavelength, spatial frequency of surface roughness, and the amplitude of surface roughness. For example, when $\lambda=0.16\ \mu m$, the 1 and 0.6 μm scale roughness will produce the large scatter of 9.2° and 15.5°, respectively, corresponding to the TIS of 3.32×10^{-1} and 3.58×10^{-1}.

IV. CONCLUSIONS

We have dealt with the nanometer characterization of diamond-turned mirrors on the micrometer and submicrometer scale in our 3D roughness measuring system based on STM. We have demonstrated the existence of the surface roughness structure on the micrometer and submicrometer scale, which can not be obtained with a conventional stylus instrument. This finer structure is one of the most important factors affecting the SPDT mirror applied in visible, EUV, and soft x-ray regions according to the calculated results of TIS and θ_d. In addition, the ASD function profile of SPDT surfaces presented by us is the basis for improving the diamond-turned surface quality.

ACKNOWLEDGMENT

We want to thank L. S. Xue for measuring the diamond-turned specimen with a Talystep profiler.

[1]J. B. Arnold, T. O. Morris, R. E. Sladky, and P. J. Steger, Opt. Eng. **16**, 324 (1977).
[2]D. L. Decker, J. M. Bennett, M. J. Soleau, J. O. Porteus, and H. E. Bennett, Opt. Eng. **17**, 160 (1978).
[3]F. E. Johnson, M. E. Curcio, D. C. Smith, and L. E. Lockett, Laser Focus, July 1981, pp. 33–36.
[4]E. L. Church and P. E. Takacs, Opt. Eng. **24**, 396 (1985).
[5]Y. Sakai, Bull. Jpn. Soc. Proc. Eng. **18**, 146 (1984).
[6]H. Eda, K. Kish, K. Nomura, H. Hashimoto, and H. Ito, Bull. Jpn. Soc. Proc. Eng. **19**, 126 (1985).
[7]C. K. Syn, Proc. SPIE **676**, 128 (1986).
[8]G. Binning, H. Rohrer, Ch. Gerber, and E. Weibel, Appl. Phys. Lett. **40**, 178 (1982).
[9]G. Binning, H. Rohrer, Ch. Gerber, and E. Weibel, Phys. Rev. Lett. **49**, 57 (1982).
[10]G. Binning, C. F. Quate and Ch. Gerber, Phys. Rev. Lett. **56**, 930 (1986).
[11]S. Alexander, L. Hellemans, O. Marti, J. Schneir, V. Elings, P. K. Hansma, M. Longmire, and J. Gurley, J. Appl. Phys. **65**, 164 (1989).
[12]R. A. Dragoset, R. D. Young, H. P. Layer, S. R. Mielczarek, E. C. Teague, and R. J. Celotta, Opt. Lett. **11**, 560 (1986).
[13]R. A. Dragoset and T. V. Vorburger, Proc. SPIE **749**, 54 (1987).
[14]J. Yu, Ph. D. dissertation, Changchun Institute of Optics and Fine Mechanics, Academia Sinica, 1993 (unpublished).
[15]J. Yu, L. Hou, J. Wei, J. E. Yao, J. L. Cao, and Y. Y. Yu, Proc. SPIE **1752**, 123 (1992).
[16]MSG-325 diamond tool lathe for micromachining of contours, Pneumo Precision, Inc.; A designer's guide to diamond machined optics, Pneumo Precision, Inc.; J. K. Myler, R. A. Parker, and A. B. Harrison, Proc. SPIE **1333**, 58 (1990).
[17]Talystep Step Height Measuring Instument, Talydata Computer, and Nanosurf-type profiler manufactured by Rank Taylor Hobson Limited, P.O. Box 36, Leicester LE47JQ, England.
[18]J. S. Bendat and A. G. Piersol, *Random Data: Analysis and Measurement Procedures* (Wiley, New York, 1971).
[19]Mathematical Group of North-East University, *Integral transformation* (High Level Education Press, Beijing, 1978) (in Chinese).
[20]P. Beckmann and A. Spizzichino, *The Scattering of Electromagnetic Waves From Rough Surfaces* (Pergamon, London, 1963).
[21]H. E. Bennett and J. O. Porteus, J. Opt. Soc. Am. **51**, 123 (1961).
[22]J. M. Bennett and L. Mattsson, *Introduction to Surface Roughness and Scattering* (Optical Society of America, Washington, DC, 1989).
[23]H. E. Bennett, Opt. Eng. **17**, 480 (1978).